

Analysis of Skin Detection Algorithms

CIS * 4720 Image Processing

Assignment 3

Darren Chay Loong

University Of Guelph

ID: 1049254

Abstract

This report aims to analyse 3 skin detection algorithms that make use of different colour spaces such as the HSV colour space, the YCrCb colour space, etc., in terms of their performance in various situations and draw conclusions based on that analysis. By implementing and testing those algorithms on several different images containing skin, we will investigate the different factors that can affect the percentage of true and false positive present in those images from each of the algorithms, as well as their general overall performance, through a qualitative, comparative and quantitative analysis of the results.

1. Introduction

Being able to detect skin in videos or pictures has become a common topic of discussion when it comes to image processing and is now used nowadays in various areas, such as facial detection. Indeed, throughout the past decades, a large variety of skin detection algorithms have been devised and refined in order to adapt to the evolving technologies and needs that we have in today's society. However, all skin detection algorithms which make use of skin colour to identify the skin regions have to tackle similar problems - choosing the right colour space and how to model the skin colour distribution in that colour space. Therefore, in an attempt to analyze how skin detection algorithms work, 3 algorithms were chosen for analysis - the Peer et al. algorithm (2003), the Chai et al. algorithm (1999), and the Wang et al. algorithm (2001) - which make use of thresholding techniques by applying several masks to an image. These 3 algorithms will be extensively tested on various images and will be visually analysed so as to judge their performance in various circumstances. Furthermore, some images will be compared to their respective ground truth images - images that already segmented out the skin regions - by using the percentage of true positive and false positive obtained from those ground truth images to see how well they were able to identify the skin regions for that image.

2. Algorithms & Metrics

2.1 Colour Spaces

Before delving into the algorithms and metrics used for the following experiments, being able to understand what some of the various colour spaces that those algorithms use is important so as to have a better idea of how the skin colour distribution is modelled in that specific colour space. Therefore, a very brief review of the colour spaces (and their properties) used in those algorithms will be done beforehand.

2.1.1 RGB Colour Space

The RGB colour space is one of the more commonly known and widely used colour spaces for storing digital image data. Combining the 3 colour channels (red, green, and blue) in varying degrees of intensity (from 0 to 255), produces a colour gamut which is known as the RGB colour space, an additive colour space. However, since this colour space does not separate chrominance from luminance, it becomes hard to isolate the chrominance from the luminance, which can make the task of skin detection harder when there are varying degrees of light intensity (brightness).

2.1.2 YCbCr Colour Space

Unlike the RGB colour space, the YC_bC_r colour space separates the luminance (Y) from the chrominance (C_b & C_r). This colour space has 3 channels, the luminance Y , constructed using a weighted sum of the RGB values, and the 2 colour difference values, C_r and C_b , that are formed by subtracting the luminance from the red and blue components of RGB (Vezhnevets et al., 2003), as seen in the following set of equations (1).

$$\begin{aligned} Y &= 0.299R + 0.587G + 0.114B \\ Cr &= R - Y \\ Cb &= B - Y \end{aligned} \tag{1}$$

2.1.3 HSV Colour Space

The HSV colour space is from the Hue-Saturation based colour spaces (HSI, HSV, HSL) which make use of 3 channels - the hue, saturation and luminance (in this case the value V). The hue identifies a colour with a part of a spectrum and is usually measured in degrees (0° - 360°), the saturation, also known as the colourfulness, refers to the relative purity or amount of white light that is mixed with the hue, and value (brightness) is how bright or dark the colour is. Both the saturation and value is usually measured in

percentage. Similar to the $Y\text{C}_b\text{C}_r$ colour space, the HSV colour space also separates the chrominance from the luminance.

2.1.4 Normalized RGB (rg chromaticity) colour space

The normalized RGB colour space, also referred to as the rg chromaticity colour space, is a 2-dimensional colour space with no intensity information (Wikipedia, 2021). This is obtained by doing a simple normalization procedure as seen in the set of equations (2). Since the sum of all 3 components is equal to 1, the third component is usually omitted to reduce the space dimensionality (Vezhnevets et al., 2003). By normalizing RGB, we reduce all variances in intensity for a colour, therefore reducing the effect of light on an object.

$$\begin{aligned} r &= \frac{R}{R + G + B} \\ g &= \frac{G}{R + G + B} \\ b &= \frac{B}{R + G + B} \end{aligned} \quad (2)$$

$$\text{And } r + g + b = 1$$

2.2 Algorithms

As discussed earlier, thresholding methods of skin segmentation require some sort of rule which will dictate the spectrum of the skin colour distribution in that specific colour space. Since most skin colours are created by a combination of red (due to blood) and yellow/brown (due to melanin), the following algorithms will attempt to identify the spectrum of colours that fall in this category in their respective colour spaces.

2.2.1 Peer et al.

The algorithm devised by Peer et al. (2003) makes use of the RGB colour space and applies 5 rules (R1 - R5) which, if all respected, implies that the current pixel falls within the spectrum of skin colours. However, there is the assumption that the images are taken under uniform daylight illumination. The rules are as follows:

$$\mathbf{R1: } R > 95 \text{ and } G > 40 \text{ and } B > 20$$

$$\mathbf{R2: } \max\{R, G, B\} - \min\{R, G, B\} > 15$$

$$\mathbf{R3: } |R-G| > 15$$

$$\mathbf{R4: } R > G$$

$$\mathbf{R5: } R > B$$

This algorithm was created by experimenting and testing several different thresholds on different training sets of pictures and choosing the threshold that gives the best results (Peer et al., 2003). Some of the things we can notice from those rules are that the pixels should be a bit more reddish (for example, R4 & R5) and that the image should not be grey-ish as well (R2). In order to implement this algorithm, after confirming that R2 is respected, each of the rules will be used to create a specific mask which will then each be applied to the image in the RGB colour space to produce a processed image with the skin sections segmented. One example of the rules being applied to an image can be seen in Fig.1 where we can see how each mask segments the image and the resulting image after applying all masks.



Fig.1 Implementation of Peer et al. algorithm on an image (from top left to bottom right) **a)** original image, **b)** applying R1, **c)** applying R3, **d)** applying R4, **e)** applying R5, **f)** processed image (applying R1-R5)

2.2.2 Chai et al.

Chai and Ngan (1999) developed an algorithm that makes use of the YC_bC_r colour space's separation of chrominance and luminance. By applying thresholds to only the chrominance components (C_b and C_r), variations in light intensity should no longer affect the results of skin detection, which should be the case for the algorithm devised by Peer et al. (2003). Based on their findings, they were able to deduce that most skin colours fall within the rules (R1 & R2) as seen below:

$$\mathbf{R1: } 77 \leq C_b \leq 127$$

$$\mathbf{R2: } 133 \leq C_r \leq 173$$

Similar to the Peer et al. algorithm (2003), the image will be converted to the YC_bC_r space and then the rules are applied to the image to create masks which will then be used to create the processed skin-segmented image. Fig.2 shows how the algorithm segments the skin regions using R1 & R2.



Fig.2 Implementation of Chai et al. algorithm on an image (from left to right) **a)** original image, **b)** applying R1, **c)** applying R2, **d)** processed image (applying R1 & R2)

2.3.3 Wang et al.

Wang and Yuan (2001) created an algorithm that makes use of 2 colour spaces in order to identify skin - the HSV and normalized RGB colour space. By using those 2 colour spaces and applying specific rules for each of those colour spaces, the spectrum of skin colours is created and should, in theory, not be affected by varying levels of brightness, since it uses 2 colour spaces that negate the effects of brightness on an image. By using both models, Wang and Yuan (2001) believe that detection is better than using only one. The rules for each of the colour spaces are as defined below (R1 & R2):

$$\mathbf{R1 \text{ (normalized RGB): } 0.36 \leq r \leq 0.465 \text{ and } 0.28 \leq g \leq 0.363}$$

$$\mathbf{R2 \text{ (HSV): } 0 \leq H \leq 50 \text{ and } 0.20 \leq S \leq 0.68 \text{ and } 0.35 \leq V \leq 1.0}$$

In order to implement that algorithm, the image is first converted to the normalized RGB space and a mask is created using R1 and the image is then converted to HSV space where the second mask is created using R2 and the resulting skin-segmented image is created by applying both masks to that image. Fig.3 shows an example of the implementation of the algorithm made by Wang et al. (2001).



Fig.3 Implementation of Wang et al. algorithm on an image (from left to right) **a)** original image, **b)** applying R1, **c)** applying R2, **d)** processed image (applying R1 & R2)

2.3 Metrics

Percentage True & False Positive

In order to quantitatively analyse the results of the experiments to be conducted, the percentage of true positive (TP) and false positive (FP) will be used to measure the effectiveness of the 3 algorithms. This will require the processed images to have a ground truth image which will be used to compare with the processed image so as to see what percentage of pixels from the processed image are actually skin pixels and what percentage are not skin pixels. This is done by applying the following equations (3) on the processed image.

$$\begin{aligned} \text{TP} &= (P_s / G_s) \times 100 \\ \text{FP} &= (P'_s / G'_s) \times 100 \end{aligned} \quad (3)$$

Where P_s is the number of true skin pixels in the processed image of size ixj , G_s is the number of skin pixels from the ground truth image, P'_s is the number of non-skin pixels in the processed image, and G'_s is $ixj - G_s$ (the difference between the number of pixels in the ground truth image and the number of skin pixels). Of course, the higher the TP value and the lower the FP value implies a better result.

3. Experiment & Results

In order to test the effectiveness of each of the 3 algorithms, a series of tests will be carried out with each algorithm and the results will then be analysed in order to draw out conclusions based on their performance. The first test that will be carried out will be an investigation of the percentage of true and false positive from each algorithm on a set of 10 different images (Fig.4) which have a ground truth image that can be used to compare with the processed images from each algorithm. The results of this test will then be analysed to have a first overview of how the algorithms perform and will then be visually analysed. Then, a more thorough analysis of the limitations of those algorithms will be tested using 4 unique types of images, as seen in Fig.5, where each image has a unique attribute that could be considered as an ‘edge case’ when it comes to image processing.



Fig.4 (From top left to bottom right) image with **a**) skin-coloured background, **b**) people with bright clothes, **c**) a bright background, **d**) warmer (yellow) colour temperature, **e**) clothes with similar colour as the skin, **f**) a dark background, **g**) people with different skin tones, **h**) varying lightning on the skin, **i**) high level of brightness, **j**) warmer (orange) colour temperature.

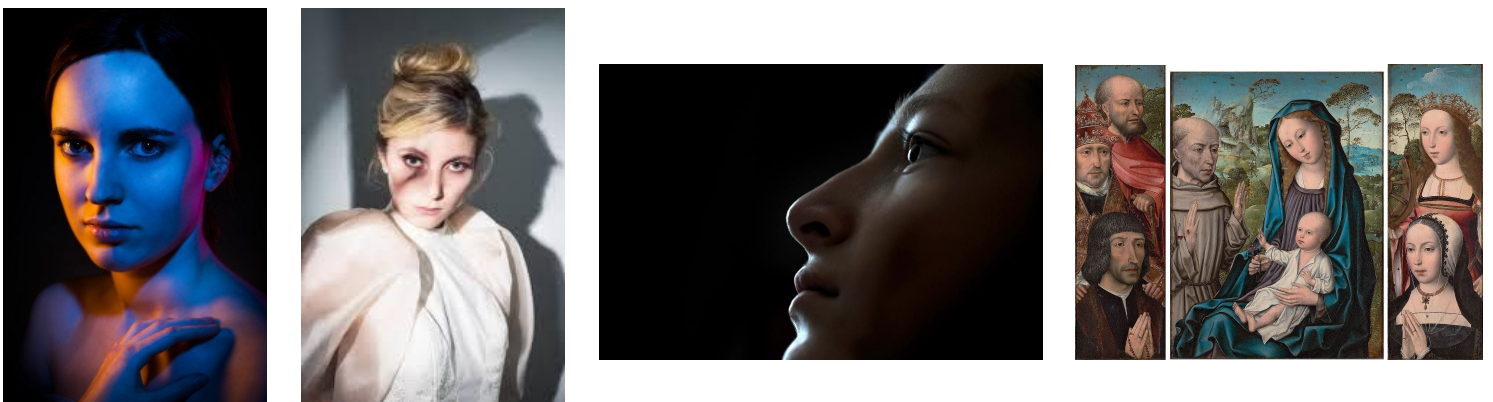


Fig.5 (From left to right) **a**) image with unusual blue-ish lighting, **b**) image with particularly bright lighting, **c**) image with really low lighting, **d**) image of a painting.

3.1 Ground Truth Image Results

After processing each of the images and obtaining the percentage TP and FP for each image for each algorithm, as seen in Table 1., the summary of the results (mean and standard deviation) was also calculated as seen in Table 2.

Table 1. Percentage of TP and FP for each processed image from each algorithm

Algorithm	% Positive	Fig.4a	Fig.4b	Fig.4c	Fig.4d	Fig.4e	Fig.4f	Fig.4g	Fig.4h	Fig.4i	Fig.4j
Peer et al.	TP	94.26	99.76	97.71	99.96	98.77	98.87	96.35	87.91	92.00	65.95
	FP	23.47	49.63	26.12	86.19	64.34	19.29	38.60	24.29	27.08	49.33
Chai et al.	TP	96.55	100	99.74	67.91	85.34	100	99.99	99.40	98.79	7.21
	FP	25.52	67.62	41.18	78.89	64.57	31.13	48.94	77.71	32.89	52.34
Wang et al.	TP	56.93	96.59	92.38	16.26	33.22	74.38	92.80	24.46	56.84	0.81
	FP	12.89	20.44	23.22	50.81	31.20	18.71	22.26	4.43	15.64	28.17

Table 2. Summary statistics obtained from Table 1.

Algorithm	Mean TP	Std Dev TP	Mean FP	Std Dev FP
Peer et al.	93.154	9.774	40.834	20.517
Chai et al.	85.493	27.863	52.079	18.478
Wang et al.	54.467	32.833	22.777	11.805

3.1.1 Quantitative Analysis of Results

At first glance, we can see that the Peer et al. algorithm produced the most reliable results in terms of correctly identifying the skin pixels since it has the highest TP average and the lowest standard deviation amongst the other 2 algorithms for the percentage TP but also had a significantly high percentage of FP which was also identified, with an average of 41%.

On the other hand, the Wang et al. algorithm produced the least reliable results in terms of skin pixel identification with the lowest TP average and highest standard deviation out of the 3 algorithms. This would imply that the performance of the Wang et al. algorithm varies widely based on the input image and usually does not do a really good job at identifying all the skin pixels (although it does get at least 50% of the skin pixels on average). However, the Wang et al. algorithm also had the lowest average FP with the least variability, meaning that it's the algorithm that does the best job of omitting any pixels which aren't skin.

The Chai et al. algorithm lies in the middle when it comes to TP performance. Although significantly better than the Wang et al. algorithm when it comes to TP (with an average that is almost 50% better than the Wang et al. algorithm), it performs the worst for FP, with the highest average of 52% (more than 2 times worse than the Wang et al. algorithm).

Thus, after performing a general quantitative analysis of the results from Table 2., we could say that Peer et al. works best if identifying skin pixels is more important than having false positives present in the result, whereas the Wang et al. algorithm works best if we are trying to minimize the percentage of false positives present in the image. However, on closer inspection, we can see that there are outliers present in the dataset from Table 1. For example, the TP values for Fig.4j was low for all 3 algorithms, especially for Wang et al. and Chai et al., or for Fig.4d, the FP values were quite high compared to the other images. Those images will be investigated further in the next section.

3.1.2 Qualitative Analysis of Results

A. Comparative Analysis

After a closer visual inspection of the results of each of the algorithms for Fig.4d, we can see that they all performed relatively poorly in removing the non-skin pixels in the image, as seen in Fig.6. This could be due to the incorrect colour balance that was present in the original image, which caused the image to appear yellowish in nature, which probably made most of the colours in the image fall within the thresholds of each of the algorithms. Furthermore, the Wang et al. algorithm actually barely kept any skin



Fig.6 Results of processing Fig.4d with the **a)** Chai et al. algorithm, **b)** Peer et al. algorithm, and **c)** Wang et al. algorithm.

pixels and instead kept more non-skin pixels, which is also reflected in Table 1. However, after correcting the colour temperature of that image, the algorithms were run again on that corrected image and the results were quite better as seen in Fig.7., where all 3 algorithms did a better job at correctly identifying the skin pixels (Fig.7c for example) and removing non-skin pixels (Fig.7b) when compared to the results from Fig.6.



Fig.7 Results of processing Fig.4d after colour temperature correction with the **a)** Chai et al. algorithm, **b)** Peer et al. algorithm, and **c)** Wang et al. algorithm.

This phenomenon is also visible in Fig.4j, where the colour temperature was also more orange-ish in nature, causing most of the algorithms to fail quite badly, except for the Peer et al. algorithm that was still able to correctly identify 66% of the skin pixels, as seen in Fig.8. Again, after preprocessing Fig.4j and correcting the colour temperature, the results are significantly better, especially for the Wang et al. algorithm, which produces the complete opposite result with barely any non-skin pixels and almost only skin pixels, as seen in Fig.9c. This shows that colour temperature plays a very important factor when applying all 3 algorithms on images and making sure that the colour temperature is correct before processing the images could yield significantly different results. One interesting thing to also note is that the Peer et al. algorithm accurately segmented the characters on the poster for Fig.4j when no preprocessing was done.



Fig.8 Results of processing Fig.4j with the **a)** Chai et al. algorithm, **b)** Peer et al. algorithm, and **c)** Wang et al. algorithm.



Fig.9 Results of processing Fig.4j after colour temperature correction with the **a)** Chai et al. algorithm, **b)** Peer et al. algorithm, and **c)** Wang et al. algorithm.

Regarding Fig.4e, which contains clothes that have similar colours to the skin, all 3 algorithms were unable to appropriately differentiate between the skin and the clothe pixels and therefore all had pretty high FP values, as seen in Fig.10. The results for this image also shows that all 3 algorithms are not sensitive enough when it comes to segmenting brown skin and brown objects or background. However, we do see less FP in the Wang et al. algorithm (Fig.10c) compared to the other 2 algorithms.

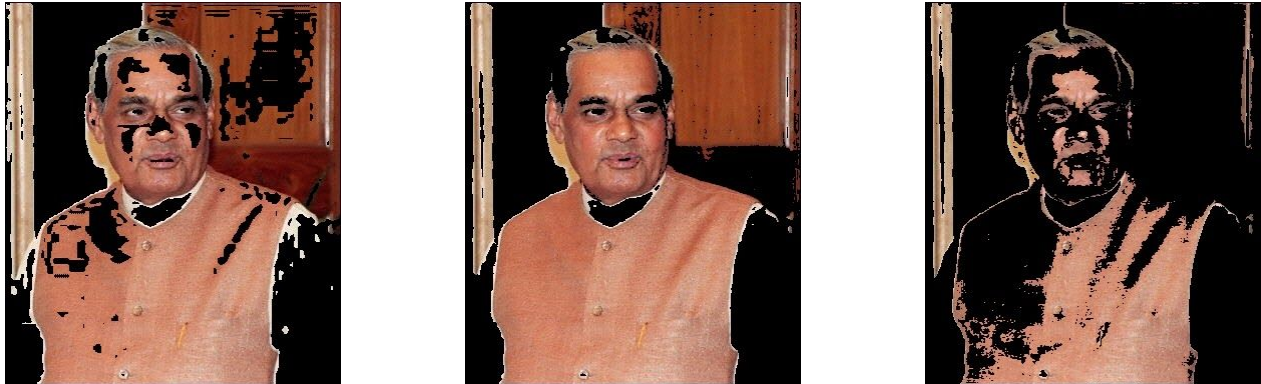


Fig.10 Results of processing Fig.4e with the **a)** Chai et al. algorithm, **b)** Peer et al. algorithm, and **c)** Wang et al. algorithm.

We can also see through the results of Fig.4c that all 3 algorithms are unable to properly remove golden-coloured pixels, as seen in Fig.11, where the golden statue was still present in all algorithms even after processing. Thus, we can also deduce that all 3 algorithms are not sensitive enough to golden colours, especially the chai et al. algorithm (Fig.11a), as well. This could also be seen in Fig.6 where the incorrect colour temperature made the image a bit golden.



Fig.11 Results of processing Fig.4c with the **a)** Chai et al. algorithm, **b)** Peer et al. algorithm, and **c)** Wang et al. algorithm.

On the other hand, we can also see through the results of Fig.4g that all algorithms can handle different skin tones pretty well. From Fig.12, without taking into consideration the percentage of FP, all algorithms correctly identified most of the skin pixels present in the image which contained both a whiter and browner skin tone. Also, we can see through Fig.12b that the Peer et al. algorithm is insensitive to red-coloured pixels as well,



Fig.12 Results of processing Fig.4g with the **a)** Chai et al. algorithm, **b)** Peer et al. algorithm, and **c)** Wang et al. algorithm.

B. Chai et al. Algorithm Analysis

The Chai et al. algorithm was insensitive to white coloured dresses, as seen in Fig.13a, and was the algorithm that had the most white-dress pixels out of all 3 of them. Interestingly, while it was insensitive to the red umbrella seen in Fig.4h (Fig.13b), it did not identify the red section of the clothes in Fig.4g (as seen in Fig.12a), nor did it identify the red poster from Fig.4j (as seen in Fig.8a). The same thing can be said for the green clothes from Fig.4f, which was identified as seen in Fig.13c but wasn't identified for the green plant in both Fig.4f and Fig.4g (as seen in Fig.12a). Therefore, we can see that there is a specific shade of red and green that this algorithm is unable to properly threshold out.



Fig.13 Results of applying the Chai et al. algorithm on **a)** Fig.4b, **b)** Fig.4h, and **c)** Fig.4f

C. Peer et al. Algorithm Analysis

One thing to note with the Peer et al. algorithm is that it was not very sensitive to yellow components as seen in Fig.14, where we can see that the yellow part of the background of Fig.4a is still present after processing.



Fig.14 Results of applying the Peer et al. algorithm on **a)** Fig.4b

D. Wang et al. Algorithm Analysis

Surprisingly, the Wang et al. algorithm did badly on Fig.4h and barely identified any skin pixels except those that were brighter due to the illumination from the sun (Fig.15a). Based on the implementation of the algorithm as discussed in section 2.3.3, this should not have been the case since this algorithm is supposed to negate the effects of varying light intensity on the image. Also, we can see from Fig.15b that this algorithm was able to properly threshold out the orange coloured hair, which wasn't the case for the other 2 algorithms, which shows that it is sensitive to orange (this is also seen in Fig.8c).

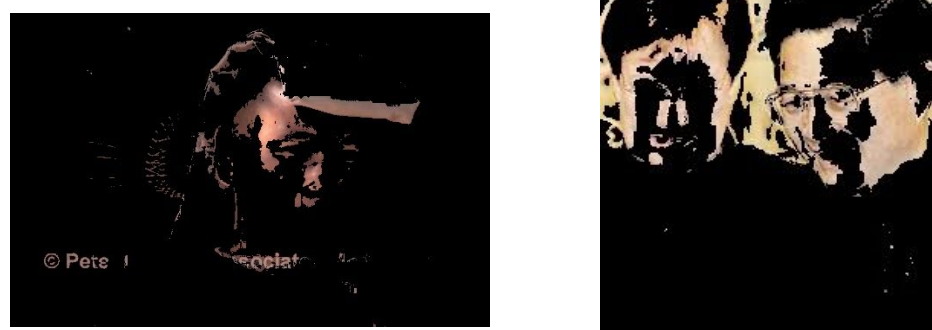


Fig.15 Results of applying the Wang et al. algorithm on **a)** Fig.4h, and **b)** Fig.4i

3.2 Unique Image Results

3.2.1 Low Lighting

After running the algorithms on this image with low lighting, the only algorithm that was able to segment out the skin was the Chai et al. algorithm. As seen in Fig.16, both the Peer et al. algorithm and the Wang et al. algorithm practically didn't detect any skin pixels except the slightly brighter contours of the face. Thus, we can conclude that the Chai et al. algorithm can still be used even in really low lighting situations.

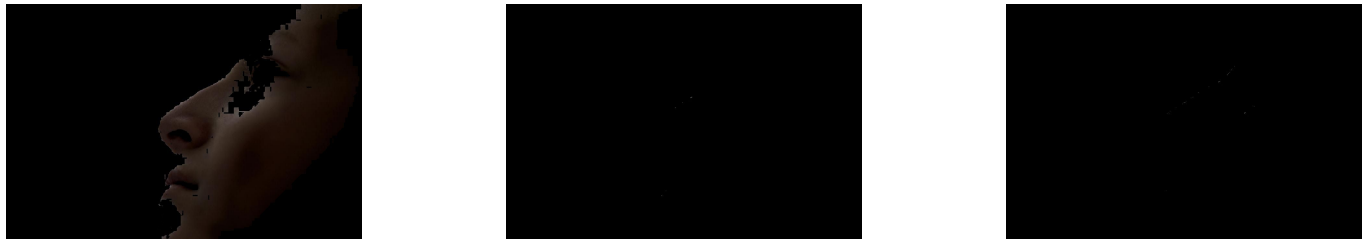


Fig.16 Results of processing Fig.5c with the **a)** Chai et al. algorithm, **b)** Peer et al. algorithm, and **c)** Wang et al. algorithm.

3.2.2 Bright Lighting

On the other hand, both the Chai et al. and Peer et al. algorithms were able to detect most of the skin pixels for the brightly lit image, as seen in Fig.17. However, while the Wang et al. algorithm did detect some skin, it did not recognize the skin pixels which were the most brightly lit (Fig.17c). This again shows that the Wang et al. algorithm is quite sensitive to brightness whereas the Chai et al. algorithm doesn't seem to be affected by lighting that much.

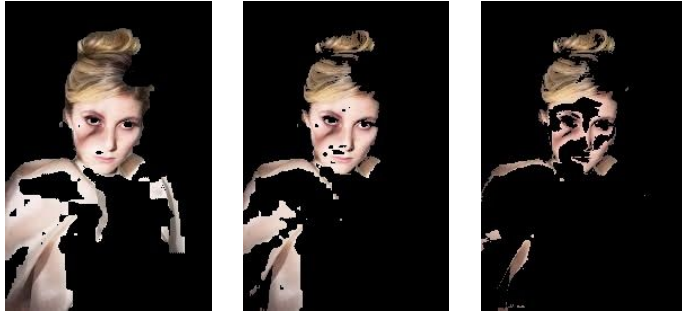


Fig.17 Results of processing Fig.5b with the **a)** Chai et al. algorithm, **b)** Peer et al. algorithm, and **c)** Wang et al. algorithm.

3.2.3 Blue-ish Lighting

After testing the algorithms with Fig.5a, it isn't too surprising that none of them was able to detect the skin pixels that were illuminated with the blue light. However, the Peer et al. algorithm was still able to detect most of the other half of the face which was illuminated with a slightly orange light (Fig.18b) and the Chai et al. algorithm detected around a quarter of the face (Fig.18a). This is not too surprising for the Peer et al. algorithm since handled Fig.4j pretty well. Again, we can see that the Wang et al. algorithm had the worst performance, barely being able to detect any skin pixels.



Fig.18 Results of processing Fig.5a with the **a)** Chai et al. algorithm, **b)** Peer et al. algorithm, and **c)** Wang et al. algorithm.

3.2.4 Painting of People

Interestingly, this time it seems that the Wang et al. algorithm had the best results with the painting as it was able to correctly identify all the skin pixels and also threshold out most of the non-skin pixels from the painting (Fig.19c). Although the other 2 algorithms were also able to detect most of the skin pixels as well, they also allowed a lot of false positives to be included in the processed image as well, especially the Chai et al. algorithm (Fig.19a).



Fig.19 Results of processing Fig.5d with the **a)** Chai et al. algorithm, **b)** Peer et al. algorithm, and **c)** Wang et al. algorithm.

4. Conclusion

After a thorough analysis of all 3 algorithms in various situations, we can see that they each have their strengths and weaknesses and cannot be used universally as an efficient skin segmentation algorithm.

The Chai et al. algorithm, while not really effective if the colour temperature of the image is warmer than usual (yellowish or orange-ish temperatures), it doesn't seem to be affected by the brightness of an image (as seen in section 3.2.1 and 3.2.2). Furthermore, the Chai et al. algorithm has the highest average percentage FP out of all 3 algorithms (Table 2.) and this could be seen through most of the figures as well (Fig.19a, Fig.12a, Fig12, etc.).

The Peer et al. algorithm is the best option if being able to identify the skin pixels is more important than having false positives also be present in the results since this was the algorithm with the highest TP. It was also the algorithm that was the least affected by colour temperature out of the 3 (Fig.7b, Fig.8b). We can also conclude that the Peer et al. algorithm has the largest skin colour distribution since it was able to accommodate unusual colour temperatures as well as unusual lighting as well (Fig.18b). However, it does seem that it does not perform well in low lighting situations (Fig.16b).

Finally, the Wang et al. algorithm seems to have the smallest skin colour distribution of the 3 algorithms. Having the lowest average TP and the lowest average FP, the Wang et al. algorithm would be the most suitable if making sure that FP are not present in the results is more important than being able to detect all the skin pixels. Also, it would seem that the Wang et al. algorithm is the most sensitive to brightness, as it performed the worst when used on images with really low or bright lighting (Fig.16c, Fig.17c), as well as colour temperature (Fig.7c, Fig.8c). Furthermore, this algorithm is particularly sensitive to orange colours (Fig.8c, Fig.15b, Fig.18c).

Thus, we can see that the Chai et al. algorithm is best suited if brightness is unusual (bright, low, or varying), the Peer et al. algorithm is best suited if percentage FP is not an issue, and the Wang et al. algorithm is best suited in removing FP, at the expense of TP. Indeed, since skin segmentation is used nowadays as one of the steps for further processing, such as facial recognition, it is important to choose the right method for the right situation. Of course, this was only a short analysis of 3 algorithms that use the thresholding technique for skin segmentation - there are several other skin segmentation techniques that are also used. However, these algorithms could be improved upon or adapted to produce better results to satisfy one's current needs.

References

- Vezhnevets, V., Sazonov, V., & Andreeva, A. (2003). A Survey on Pixel-Based Skin Color Detection Techniques. *Proc. Graphicon*, 85–92. <https://doi.org/10.1.1.189.545>
- Wikimedia Foundation. (2021, March 17). *Rg chromaticity*. Wikipedia. https://en.wikipedia.org/wiki/Rg_chromaticity.
- Solina, F., Peer, P., Batagelj, B., & Juvan, S. (2003). 15 seconds of fame - an interactive, computer-vision based art installation. *7th International Conference on Control, Automation, Robotics and Vision, 2002. ICARCV 2002*. <https://doi.org/10.1109/icarcv.2002.1234820>
- Chai, D., & Ngan, K. N. (1999). Face segmentation using skin-color map in videophone applications. *IEEE Transactions on Circuits and Systems for Video Technology*, 9(4), 551–564. <https://doi.org/10.1109/76.767122>
- Wang, Y., & Yuan, B. (2001). A novel approach for human face detection from color images under complex background. *Pattern Recognition*, 34(10), 1983–1992. [https://doi.org/10.1016/s0031-3203\(00\)00119-9](https://doi.org/10.1016/s0031-3203(00)00119-9)